



Published in final edited form as:

Vis Comput. 2016 November ; 32(11): 1499–1506. doi:10.1007/s00371-015-1152-5.

Dynamic 3-D computer graphics for designing a diagnostic tool for patients with schizophrenia

Attila Farkas¹, Thomas V Papathomas^{1,2}, Steven M Silverstein³, Hristiyan Kourtev⁴, and John F Papayanopoulos⁵

¹Laboratory of Vision Research/Center for Cognitive Science, Rutgers University

²Department of Biomedical Engineering, Rutgers University

³Division of Schizophrenia Research, Rutgers University Behavioral HealthCare and Robert Wood Johnson Medical School Department of Psychiatry, Rutgers Biomedical and Health Sciences

⁴Center for Cognitive Science, Rutgers University

⁵College of Engineering, Georgia Institute of Technology

Abstract

We introduce a novel procedure that uses dynamic 3-D computer graphics as a diagnostic tool for assessing disease severity in schizophrenia patients, based on their reduced influence of top-down cognitive processes in interpreting bottom-up sensory input. Our procedure uses the hollow-mask illusion, in which the concave side of the mask is misperceived as convex, because familiarity with convex faces dominates sensory cues signaling a concave mask. It is known that schizophrenia patients resist this illusion and their resistance increases with illness severity. Our method uses virtual masks rendered with two competing textures: (a) realistic features that enhance the illusion; (b) random-dot visual noise that reduces the illusion. We control the relative weights of the two textures to obtain psychometric functions for controls and patients and assess illness severity. The primary novelty is the use of a rotating mask that is easy to implement on a wide variety of portable devices and avoids the use of elaborate stereoscopic devices that have been used in the past. Thus our method, which can also be used to assess the efficacy of treatments, provides clinicians the advantage to bring the test to the patient's own environment, instead of having to bring patients to the clinic.

Keywords

3-D computer graphics; visual illusion; perception; schizophrenia; clinical diagnosis

1 Introduction

Well-established evidence from a long series of empirical cognitive neuroscience studies indicates that visual stimulation can now be employed to test the extent of perceptual impairment caused by mental disorders [1-3]. The idea of using computer graphics to generate visual stimulation for therapy and rehabilitation is not new [4, 5]. For example, multi-modal virtual environments and graphical displays offer benefits for improving

physical skills and abilities [6-10]. Yet, advances of computer graphics have not been fully utilized for testing serious mental disorders, even though analysis of perceptual responses to visual inputs such as the Rorschach inkblot test has been used to examine personality characteristics and emotional functioning. The present paper discusses the possibilities of using computer-generated visual animations to examine how the engagement of top-down processes, such as stored knowledge of faces, in the interpretation of sensory input differs between schizophrenia patients and controls. Specifically, we use computer-generated animations of 3-D virtual objects to explore taking a step toward designing a portable computerized testing procedure for schizophrenia patients.

2 Background

2.1 Impaired visual information processing in schizophrenia

Schizophrenia affects about 1% of the population. It is a psychiatric disorder characterized by hallucinations, disorganized thought, delusions, and a decline in both mental and physical functioning. While it has been difficult to pinpoint cognitive mechanisms that are directly related to schizophrenia [11], there may be a specific deficit in information processing that can be useful in characterizing the severity of the illness. This particular deficit affects visual cognition and results in fragmented perception of objects. Research on disturbances of perceptual organization (PO) related to schizophrenia has a long history. Early investigations [12, 13] argued that deficits in organizing elements into whole objects are perhaps one of the most significant indicators of the disorder. As empirical investigations with a wide range of approaches accumulated over the years [14-18], a possible link between perceptual organization and schizophrenia emerged. Research provided solid evidence that deficit in PO is specific to schizophrenia, but not significant in other psychiatric disorders [19-21]. In recent years, advances in cognitive neuroscience revealed that visual information processing deficits might also be related to inadequate communication between cognitive, top-down, functions that are interpreting the bottom-up, data-driven visual input [1-3]. Specifically, disturbed mediation between the two streams of visual information flow (bottom-up/top-down processes) is indicated by the lack of top-down control in patients with schizophrenia [21, 2, 22, 23].

2.2 Visual information processing and visual illusions

Literature on vision suggests that visual perception is the product of the dynamic interaction of top-down and bottom-up processes. Bottom-up, or data-driven, processes utilize information derived directly from the sensory organs, such as the eyes. Top-down, or knowledge-based, cognitive, processes interpret the sensory input based on expectations and stored knowledge. To perceive the surrounding environment as a meaningful whole, the interactions between bottom-up and top-down processes need to be fully operational. Visual illusions provide a useful tool to examine the dynamic interplay between cognitive processes and the sensory input. Perhaps one of the best-known visual illusions is the hollow-face illusion, which is a form of depth-inversion illusion (DII) where the hollow (concave) parts of the object are misperceived as convex and vice versa. The illusion is so powerful that even viewers who are fully aware of the true global concave shape of the mask perceive it as convex. The hollow-face illusion provides some of the most convincing evidence for the

influence of top-down knowledge on the visual input [24-28]. Namely, lifelong familiarity with convex faces dominates over robust data-driven sensory signals that would elicit a concave percept, such as binocular disparity (stereoscopic) and motion parallax signals, and produces the final illusory convex percept. However, not everyone perceives a strong hollow-mask illusion. It is known that people with schizophrenia tend to perceive the true shape of the concave mask [2, 3, 24, 29]. A previous investigation used dynamic causal modeling to analyze fMRI (functional Magnetic Resonance Imaging) data of control volunteers and schizophrenia patients [2]. This procedure provided a successful way to analyze how different brain areas interact with each other during the observation of a concave mask. The analysis indicated that top-down processes were weaker and bottom-up processes were stronger in patients than in healthy controls while perceiving hollow-mask stimuli [2].

In addition, research on DII showed that visual top-down driven processes are impaired already in the early stages of schizophrenia [3]. A more recent study on DII analyzed convexity judgments on physically concave scenes and faces of 30 schizophrenia patients and 25 controls [29]. Data indicated that patients experienced fewer depth-inversion illusions than healthy controls for both faces and scenes. Most importantly, the study revealed that the frequency of veridical percepts of a concave object is correlated with more positive symptoms and the need of structured treatment. The above studies suggest that perceptual responses to a concave mask may serve as a state marker for schizophrenia.

2.3 Textural information and the hollow-face illusion

There have been numerous studies on the hollow-mask illusion that provided valuable information on how texture, shading and position influence the strength of the illusory percept [1, 25, 29, 30, 31]. Modifying the texture of the mask can either enhance or completely break down the illusion, depending on the nature of the texture. The effect of textural information was demonstrated in an early experiment that employed physical models of a concave mask [25, 30]. In the experiment, stereo pairs were obtained after projecting a random-dot texture onto a physical hollow mask. Results showed variations in perceptual experiences as a function of the contrast of the random-dot texture. When the random-dot texture contrast was low, the illusion was strong but the illusion disappeared at high contrasts. These results demonstrated the importance of depth cues provided by the fine details of the texture. The effect of textural noise on the hollow-mask illusion was also demonstrated in a more recent experiment [1]. In summary, a random noise texture is capable of providing sufficient data-driven stereoscopic depth cues to perceive the true concave 3-D mask shape, thus overcoming the visual system's top-down influence of past experience with convex faces.

On the other end, another experiment employing physical models of hollow scenes and faces demonstrated the effect of realistic painting [29]. Realistically painted facial features strengthen the illusion by providing additional cues (painted lips, eyes, eyebrows, etc.) that make the mask more familiar and recognizable as a face when compared to a uniformly painted mask. Based on this familiarity, top-down processes will act on the visual input and enhance the illusion. As a result observers will experience the painted concave mask to be a normal convex face [29]. The two extreme renderings provide the two extreme conditions,

with the random-dot texture strongly favoring the true (veridical) concave percept, and the realistic feature texture enhancing the convex (illusory) percept.

3 Illusory motion and the hollow-face illusion

To provide binocular depth information about the 3-D structure of the mask, previous investigators obtained stereoscopic pairs of images by projecting a random-dot stereogram either onto physical masks [25, 30] or onto virtual masks [1]. Experiencing the hollow-mask illusion with stereo viewing under ideal conditions, where each eye views the image intended for it, without any interference from the other eye's image, requires elaborate haploscopes or time-multiplexing electronic hardware, such as Stereographics Corporation's liquid-crystal diode (LCD) shutter goggles CrystalEyes® [1]. One may use red-green anaglyphs and matching red-green glasses as an inexpensive alternative but there may be undesirable "cross-talk" in that a faint version of one eye's image "leaks" into the other eye's input. A recent investigation established that monocular motion cues are as effective as binocular stereoscopic cues in testing for differences between schizophrenia patients and controls with respect to the strength of the illusion [29]. Since the target population of schizophrenia patients for the proposed technique requires short durations for the examination procedure, our goal is to reduce the length of testing and to simplify the required equipment. To avoid shutter glasses and stereo rendering, our method uses motion to provide information on 3-D depth. Adding kinetic information and avoiding stereoscopic displays eliminates the required hardware. The kinetic depth effect (KDE) refers to the ability of the visual system to recover the three-dimensional shape of an object from viewing that object as it rotates [32, 33]. The KDE can be manipulated by changing the parameters of rotational amplitude θ and speed ω . For example, a condition with $\theta = 0$ involves viewing a stationary hollow mask from only one perspective (see Fig. 2b) and could result in 100% illusory percept, because there are no cues to perceive the stationary mask as concave. Increasing θ can provide useful depth-from-motion, or KDE, cues about the veridical concave structure of the object, thus breaking the illusion. Similarly, varying the value of the rotational speed ω can have an effect on the illusion strength, as explained in a later section.

When viewing a rotating 3-D mask, the visual system has instant access to bottom-up, data-driven, depth-from-motion cues to recover the veridical structure of the object. Nevertheless, it is known that when observers view a rotating hollow mask, they often perceive a convex (illusory) face rotating in the opposite direction, presumably because of top-down, face-familiarity cues [26, 34]. Thus, perceptual responses to the rotating hollow mask can provide valuable information on how top-down processes are used to interpret sensory visual input. In our method we combine the KDE and the effect of textural information on the hollow-mask illusion into a single testing procedure that uses virtual 3-D masks for patients with schizophrenia. The advantages of virtual stimuli are obvious, since it is extremely difficult, if not impossible, to apply precise control for the proportions of textural information.

4 Computer graphics and the clinical use of the hollow-face illusion

Virtual masks have already been employed to measure confidence ratings of perceived convexity/concavity [1]. During the procedure, realistic facial features competed with

random noise, as they were both mapped onto the surface of the hollow virtual mask in various proportions. The resulting stimuli were presented to the viewers as stereo pairs. Results showed that the frequency of veridical responses varied as a function of the proportion of noise texture [1]. Our method uses the KDE because this procedure has a distinct advantage over stereo viewing. Namely, the KDE procedure can be implemented on iPads® or similar simple display devices, that allow clinicians to carry the test to the patient's environment, rather than bring the patient to the clinic. This is extremely desirable, given the difficulties experienced by practicing clinicians to schedule reliable visits by schizophrenia patients.

5 Methods

5.1 Materials

The face geometry was generated by a 3-D face-generating modeling middleware called FaceGen®. The program includes algorithms to modify apparent ethnicity, age and gender (e.g. extremely masculine, extremely feminine). These options provide a valuable asset to control over observer gender bias. As a final output, FaceGen generates the 3-D mesh data of a human head. The head can be exported in OBJ format and the realistic facial texture as a JPG image file. For our purposes, we have generated a gender-neutral head with "average" skin color defined as a mixed color of all races. Since the output object is a complete head (Fig. 1a) a modification was required to create the final hollow-mask stimuli. The head object was imported into Blender®, an open-source 3-D modeling software. To model a physical hollow mask, the mesh of the head was divided into two parts using a coronal plane, as shown in Fig. 1b and the face part was simplified by reducing the number of polygons.

As a final step, the edges of the facial mask were smoothed and cleaned up from remaining loose vertices and polygons. All surface normals were flipped to reverse the direction of the faces so as to avoid rendering and lighting problems of the hollow side. The final model consisted of approximately 6,000 polygons (Fig. 2).

Two types of textural information were mapped onto the surface of 3-D mask object. (1) The face and skin texture, imgF, that was generated by Facegen and included realistic facial features; (2) a random-dot texture, imgR, that was generated in MATLAB. A rim with the color of yellow was mapped on the perimeter of the mesh to provide additional information about the 3-D structure. Texture mapping was accomplished in Blender®. To ensure an approximately uniform density of random dots on the 3-D surface of the mask, we followed with a manual editing of the UV map, which is a modified coordinate system that allows the manipulation of textural mapping onto the 3-D geometry of the mask (Fig. 3). A modification of a MATLAB program [35] was used to render the 3-D mask object. The program is designed to load in any OBJ file and to read in texture coordinates from the related material file (MTL). The code controls the setup of Psychophysics Toolbox [36-38] for OpenGL 3-D rendering support and visualizes the mesh in 3-D space. Lighting is generated from a directional light source positioned in front of the object with a relative intensity of 1. The MATLAB program also allows the rotation of the object by an angle of the desired magnitude θ and a rotational speed ω . We used a vertical axis of rotation located

at the centroid of the mask. The virtual camera was positioned in front of the origin of the coordinate system. The realistic-feature texture imgF and the random-dot texture imgR were mapped onto the surface by using the same UV coordinates previously defined in Blender®. The texture titration is accomplished by assigning weights F and R for modulating the contrast of the two component images into a composite image imgC , where each pixel (i,j) of imgC is given by

$$\text{imgC}(i,j) = F * \text{imgF}(i,j) + R * \text{imgR}(i,j),$$

where $0 \leq F \leq 1$ and $R = 1-F$. We gradually transformed the face rendering from a purely random texture ($F=0$) to a purely featural texture ($F=1$) by titrating the two components (Fig. 4).

The strength of the illusory effect depends on at least three factors: (a) On the rotational amplitude θ ; (b) on the speed of rotation ω ; (c) on the relative weights of the figural texture F and the random-dot texture $R=(1-F)$. Specifically: (a) The strength of the illusion is expected to decrease as θ increases because of increased bottom-up motion cues that help viewers recover the veridical concave shape. (b) The illusion strength is also expected to decrease as the rotational speed ω increases. This is expected, given the time delays in triggering top-down processes for perceiving 3-D shape and for recognizing objects [39]. Increasing ω restricts the amount of time the visual system has to engage top-down processes, thereby decreasing the illusion strength. (c) Finally, the presence of significant visual noise texture for low values of F provides the visual system with strong bottom-up motion-driven depth cues that weaken the illusion.

5.2 Procedure - Results

Subjects—The subject sample consisted of 14 (4 females, 10 males) healthy subjects. All participants consented and received monetary compensation for their time. Subjects' age ranged between 18 and 66 years. All subjects had normal-or-corrected to normal vision.

Stimuli—Supplementary online material for stimulus animation and objects are in (https://dl.dropboxusercontent.com/u/1627117/KDE_Visual_computer/home.html). The same object geometry was utilized in each trial with the following values of F (weight of realistic texture): 0%, 15%, 25%, 35%, 50%, 77%, and 100%. The maximum width and height of the mask object were 18.5 cm and 30 cm, respectively (measured on the screen). Each of the 7 stimuli was presented oscillating with fixed $\omega=0.05^\circ/\text{second}$ and fixed amplitude $\theta=18^\circ$. The value θ was selected to avoid self-occlusion, which could provide additional depth cues for the observer. The value for ω was selected to avoid motion blur.

Procedure—At the beginning of the experiment, subjects were shown a physical sample stimulus up close—a realistically painted mask that was convex on one side and concave on the other. Participants were told that they would see a similar animated 3-D object on a computer screen, and that—while observing the stimulus—they would indicate with a key press whether the object appeared to be “popping out” (convex) or “caving in” (concave).

In each of the 7 experimental trials, participants were seated in front of an ASUS VG278 LCD monitor with a resolution of 1920×1080 and refresh rate of 60 Hz. The viewing distance for each subject was approximately 100 cm. Participants provided their responses on a keyboard by pressing the up arrow key (if they perceived the mask as “caving in”) or the down arrow key (if they perceived the mask as “popping out”). In each trial, subjects were prompted to indicate their dominant percept (concave/convex) 5 seconds after the stimulus onset. A trial lasted for 120 seconds, during which subjects indicated the changes in their perceptual experience (from concave to convex and vice versa). Participants’ responses were collected by a program that calculated the fraction of total time spent in the illusory percept (proportion illusory response). Between trials, subjects received a 10-second break. The seven mask objects were presented in a Latin square design so that each participant was exposed to the stimuli in a different order.

Results—Participants rated the stimulus with $F = 100\%$ as convex on average 85.5% of the time, which is significantly different from the convexity rating of the stimulus with $F=0\%$, which was rated to be convex 24.4% on average ($t(13) = 6.392, p < .000; d=3.416$). Between-subject variability of convexity ratings indicates the highest confidence in the $F=100\%$ condition with $\sigma = 0.2455$. A one-way analysis of variance revealed an effect of the weight F on the proportion illusory response, $F(6,13) = 5.473, p < .000$. The dependence of the strength of the illusory effect on the amount of textural information is depicted in Fig. 7.

We also conducted preliminary experiments with a different set of 5 observers to explore how the illusion strength depends on the rotational amplitude θ and the rotational speed ω . As expected, illusion strength decreased monotonically with increasing θ , ultimately breaking down when θ was adequately large to cause self-occlusion. The dependence of illusion strength on rotational speed ω was not as clear as that of θ , but the predicted pattern of decreasing illusion strength with increasing ω was generally obtained.

6 Conclusions

6.1 Perceptual experiences and KDE

The strength of the illusory effect was observed to depend on at least three factors: (a) It decreased as the rotational amplitude θ of the hollow mask increased, as indicated schematically in Fig. 6a, because of increased bottom-up motion cues that help viewers recover the veridical concave shape. (b) The illusion strength also decreased as the rotational speed ω increased (shown schematically in Fig. 6b), as expected, given the time delays in triggering top-down processes for recovering 3-D shape and object recognition [39]. Increasing ω restricts the amount of time the visual system has to engage top-down processes, thereby decreasing the illusion strength. (c) Finally, the presence of increasing visual noise texture provides the visual system with stronger bottom-up motion-driven depth cues that progressively weaken the illusion (Fig. 6c). The above observations enable experimenters to manipulate θ , ω and F for obtaining a wide range of conditions to test for differences between schizophrenia patients and controls. The present experiment manipulated only F to obtain a set of stimuli that range from a very *weak* illusion for $F=0$ (albeit not the *weakest* illusion) to a very strong illusion for $F=1$ (not the *strongest* illusion).

In future studies, we plan to manipulate θ and ω , in addition to F , to obtain two extreme optimal conditions. The two extreme optimal conditions are characterized by a stable perceptual experience where the observer stays in either the veridical or the illusory percept nearly 100% of the time during the stimulus presentation. For example, with appropriately selected amplitude and rotational speed and $F=0\%$, the observer should report the true shape (concave) of the masks all the time during the 2-minute trial. In order to define optimal presentation conditions, further investigations are needed to characterize how appropriate values for F , θ and ω are selected so that the dynamic presentation provides a set of stimuli that result in a range of monotonically changing percepts, starting with a stimulus that is perceived as strongly concave at one extreme and ending with a stimulus that results in a strongly convex percept, with appropriate stimuli in the set that result in intermediate percepts.

6.2 Benefits of a computerized testing procedure

The advantage of the dynamic presentation compared to static stereoscopic images or to physical masks is that it does not require elaborate stereo apparatus or stereo glasses for 3-D stimulus presentation, or precisely controlled lighting of physical masks. In addition, when conducting experiments with physical stimuli, it takes considerable time to transition from one trial (one mask stimulus) to the next trial (involving a different mask). It involves physically placing an occluder in front of the stimulus, asking observers to close their eyes, mounting the new mask onto the presentation apparatus, and then removing the occluder to uncover the mask for the observer to view. These steps take about 60-80 seconds, as compared to a computerized presentation that takes less than 5 seconds. Hence the administration of the computerized test does not require extended periods of time and it can be conducted wherever the patient is located. Our KDE method is suitable as a procedure that can run on multiple portable platforms such as laptops, electronic tablets or even smart phones. The collected data can be instantly uploaded to the Internet and analyzed by a therapist. In addition to its diagnostic value, the system can also be used to assess the efficacy of therapeutic or pharmaceutical treatments, based on our previous findings that the strength of the illusion correlates with the severity of the illness [40].

References

1. Hill H, Johnston A. The hollow-face illusion: Object-specific knowledge, general assumptions or properties of the stimulus? *Perception*. 2007; 36(2):199–223. doi:10.1068/p5523. [PubMed: 17402664]
2. Dima D, Roiser JP, Dietrich DE, Bonnemann C, Lanfermann H, Emrich HM, Dillo W. Understanding why patients with schizophrenia do not perceive the hollow-mask illusion using dynamic causal modelling. *Neuroimage*. 2009; 46(4):1180–1186. doi:10.1016/j.neuroimage.2009.03.033. [PubMed: 19327402]
3. Dima D, Dietrich DE, Dillo W, Emrich HM. Impaired top-down processes in schizophrenia: a DCM study of ERPs. *Neuroimage*. 2010; 52(3):824–832. doi:10.1016/j.neuroimage.2009.12.086. [PubMed: 20056155]
4. Liarokapis F. Special issue on Serious Games and Virtual Worlds. *Visual Comput*. 2009; 25(12): 1053–1054. doi:10.1007/s00371-009-0390-9.
5. Kang KK, Kim JA, Kim D. Development of a sensory gate-ball game system for the aged people. *Visual Comput*. 2009; 25(12):1073–1083. doi:10.1007/s00371-009-0385-6.

6. Moya S, Grau S, Tost D. The wise cursor: assisted selection in 3D serious games. *Visual Comput.* 2013; 29(6-8):795–804. doi:10.1007/s00371-013-0831-3.
7. Jafri R, Ali SA, Arabnia HR, Fatima S. Computer vision-based object recognition for the visually impaired in an indoors environment: a survey. *Visual Comput.* 2014; 30(11):1197–1222. doi: 10.1007/s00371-013-0886-1.
8. Burke JW, McNeill MDJ, Charles DK, Morrow PJ, Crosbie JH, McDonough SM. Optimising engagement for stroke rehabilitation using serious games. *Visual Comput.* 2009; 25(12):1085–1099. doi:10.1007/s00371-009-0387-4.
9. Farkas AJ, Hajnal A, Shiratuddin MF, Szatmary G. A Proposed Treatment for Visual Field Loss caused by Traumatic Brain Injury using Interactive Visuotactile Virtual Environment. *Innovations in Computing Sciences and Software Engineering.* 2010:495–498. doi: 10.1007/978-90-481-9112-3_84.
10. Crosbie JH, Lennon S, McNeill MDJ, McDonough SM. Virtual reality in the rehabilitation of the upper limb after stroke: The user’s perspective. *Cyberpsychol Behav.* 2006; 9(2):137–141. doi:DOI 10.1089/cpb.2006.9.137. [PubMed: 16640466]
11. Carter CS. Applying new approaches from cognitive neuroscience to enhance drug development for the treatment of impaired cognition in schizophrenia. *Schizophrenia Bull.* 2005; 31(4):810–815. doi:10.1093/schbul/sbi046.
12. Chapman J. The early symptoms of schizophrenia. *Br J Psychiatry.* 1966; 112(484):225–251. [PubMed: 4957283]
13. Wells DS, Leventhal D. Perceptual grouping in schizophrenia: replication of Place and Gilmore. *J Abnorm Psychol.* 1984; 93(2):231–234. [PubMed: 6725757]
14. Frith, CD. *The cognitive neuropsychology of schizophrenia. Essays in cognitive psychology.* L. Erlbaum Associates, Hove, UK; Hillsdale, USA: 1992.
15. Knight RA, Silverstein SM. A process-oriented approach for averting confounds resulting from general performance deficiencies in schizophrenia. *Journal of Abnormal Psychology.* 2001; 110(1):15–30. doi:Doi 10.1037/0021-843x.110.1.15. [PubMed: 11261389]
16. Rabinowicz EF, Opler LA, Owen DR, Knight RA. Dot enumeration perceptual organization task (DEPOT): Evidence for a short-term visual memory deficit in schizophrenia. *Journal of Abnormal Psychology.* 1996; 105(3):336–348. [PubMed: 8772004]
17. Silverstein S, Uhlhaas PJ, Essex B, Halpin S, Schall U, Carr V. Perceptual organization in first episode schizophrenia and ultra-high-risk states. *Schizophr Res.* 2006; 83(1):41–52. doi:10.1016/j.schres.2006.01.003. [PubMed: 16497484]
18. Silverstein SM, Keane BP. Vision Science and Schizophrenia Research: Toward a Re-view of the Disorder Editors’ Introduction to Special Section. *Schizophrenia Bull.* 2011; 37(4):681–689. doi: 10.1093/schbul/sbr053.
19. Doniger GM, Foxe JJ, Murray MM, Higgins BA, Javitt DC. Impaired visual object recognition and Dorsal/Ventral stream interaction in schizophrenia. *Arch Gen Psychiat.* 2002; 59(11):1011–1020. doi:DOI 10.1001/archpsyc.59.11.1011. [PubMed: 12418934]
20. Foxe JJ, Murray MM, Javitt DC. Filling-in in schizophrenia: A high-density electrical mapping and source-analysis investigation of illusory contour processing. *Cereb Cortex.* 2005; 15(12):1914–1927. doi:10.1093/cercor/bhi069. [PubMed: 15772373]
21. Schenkel LS, Spaulding WD, Silverstein SM. Poor premorbid social functioning and theory of mind deficit in schizophrenia: evidence of reduced context processing? *J Psychiat Res.* 2005; 39(5):499–508. doi:10.1016/j.jpsychires.2005.01.001. [PubMed: 15992559]
22. Gold JM, Fuller RL, Robinson BM, Braun EL, Luck SJ. Impaired top-down control of visual search in schizophrenia. *Schizophr Res.* 2007; 94(1-3):148–155. doi:10.1016/j.schres.2007.04.023. [PubMed: 17544632]
23. Koethe D, Kranaster L, Hoyer C, Gross S, Neatby MA, Schultze-Lutter F, Ruhrmann S, Klosterkötter J, Hellmich M, Leweke FM. Binocular depth inversion as a paradigm of reduced visual information processing in prodromal state, antipsychotic-na < ve and treated schizophrenia. *Eur Arch Psy Clin N.* 2009; 259(4):195–202. doi:10.1007/s00406-008-0851-6.

24. Schneider U, Borsutzky M, Seifert J, Leweke FM, Huber TJ, Rollnik JD, Emrich HM. Reduced binocular depth inversion in schizophrenic patients. *Schizophr Res.* 2002; 53(1-2):101–108. [PubMed: 11728843]
25. Georgeson MA. Random-dot stereograms of real objects: observation on stereo faces and moulds. *Perception.* 1979; 8(5):585–588. [PubMed: 503788]
26. Gregory, RL. *The intelligent eye.* Weidenfeld & Nicolson; London: 1970.
27. Klopfer DS. Apparent Reversals of a Rotating Mask - a New Demonstration of Cognition in Perception. *Percept Psychophys.* 1991; 49(6):522–530. doi:Doi 10.3758/Bf03212186. [PubMed: 1857626]
28. Papathomas TV, Bono LM. Experiments with a hollow mask and a reverspective: Top-down influences in the inversion effect for 3-D stimuli. *Perception.* 2004; 33(9):1129–1138. doi:10.1068/p5086. [PubMed: 15560511]
29. Keane BP, Silverstein SM, Wang YS, Papathomas TV. Reduced Depth Inversion Illusions in Schizophrenia Are State-Specific and Occur for Multiple Object Types and Viewing Conditions. *Journal of Abnormal Psychology.* 2013; 122(2):506–512. doi:10.1037/a0032110. [PubMed: 23713504]
30. Yellott JI, Kaiwi JL. Depth inversion despite stereopsis: The appearance of random-dot stereograms on surfaces seen in reverse perspective. *Perception.* 1979; 8(2) doi:10.1068/p080135471677.
31. Van den Enden A, Spekreijse H. Binocular depth reversals despite familiarity cues. *Science.* 1989; 244(4907):959–961. doi:10.1126/science.2727687 2727687. [PubMed: 2727687]
32. Wallach H, O'Connell DN. The kinetic depth effect. *Journal of Experimental Psychology.* 1953; 45(4):205–217. doi:10.1037/h0056880 13052853. [PubMed: 13052853]
33. Ullman, S. Massachusetts Inst of Technology Pr; England, *The interpretation of visual motion.* Oxford; England: 1979. *The interpretation of visual motion;* p. 229
34. Papathomas TV. Art pieces that 'move' in our minds - an explanation of illusory motion based on depth reversal. *Spatial Vision.* 2008; 21(1-2):79–95. doi:Doi 10.1163/156856808782713852.
35. Vuong, QC. [Accessed May 18 2014] MorphDemo. 2010. http://ftp.tuebingen.mpg.de/pub/pub_dahl/stmdev10_D/Matlab6/Psychtoolbox/PsychDemos/OpenGL4MatlabDemos/MorphDemo/MorphDemo.m
36. Brainard DH. The psychophysics toolbox. *Spatial Vision.* 1997; 10(4):433–436. doi:Doi 10.1163/156856897x00357. [PubMed: 9176952]
37. Kleiner M, Brainard D, Pelli D. What's new in Psychtoolbox-3? *Perception.* 2007; 36:14–14.
38. Pelli DG. The VideoToolbox software for visual psychophysics: Transforming numbers into movies. *Spatial Vision.* 1997; 10(4):437–442. doi:Doi 10.1163/156856897x00366. [PubMed: 9176953]
39. Bar M, Kassam KS, Ghuman AS, Boshyan J, Schmidt AM, Dale AM, Hamalainen MS, Marinkovic K, Schacter DL, Rosen BR, Halgren E. Top-down facilitation of visual recognition (vol 103, pg 449, 2006). *P Natl Acad Sci USA.* 2006; 103(8):3007–3007. doi:10.1073/pnas.0600325103.
40. Nuechterlein KH, Dawson ME, Green MF. Information-Processing Abnormalities as Neuropsychological Vulnerability Indicators for Schizophrenia. *Acta Psychiat Scand.* 1994; 90:71–79. doi:DOI 10.1111/j.1600-0447.1994.tb05894.

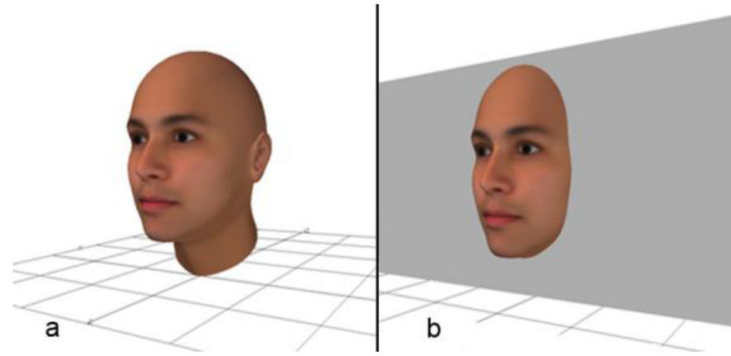


Fig. 1.
(a) The human head mesh loaded into Blender (b) the head object was divided into two parts using a coronal plane

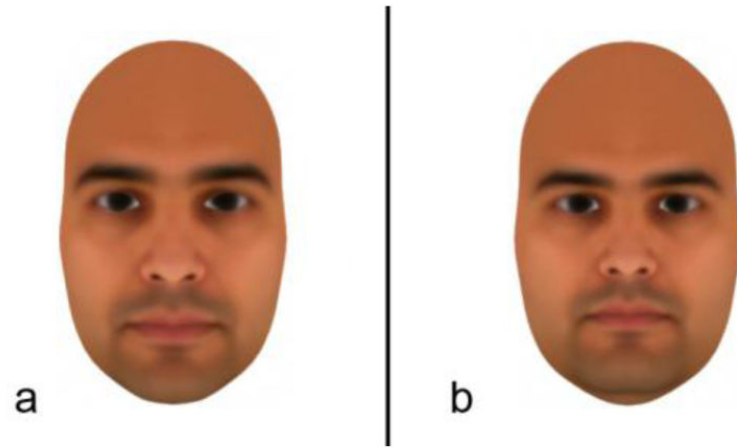


Fig. 2.
(a) Convex side of the final mask model (b) Concave side of the model



Fig. 3.
The “net” represents the UV texture map. The net consists of triangles; the area of each triangle can be increased/decreased individually

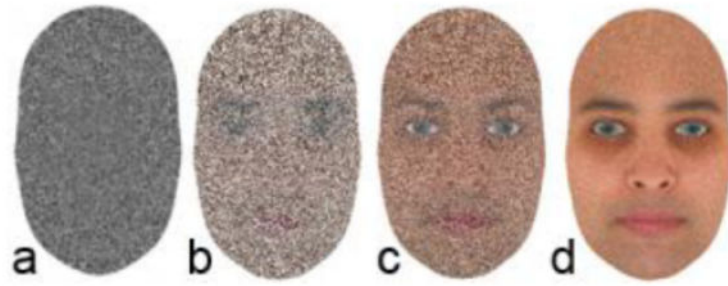


Fig. 4.
Examples of texture titration (a) $F=0\%$. (b) $F=25\%$. (c) $F=50\%$. (d) $F=85\%$

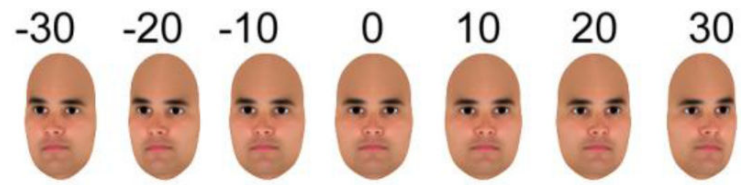
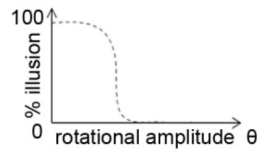
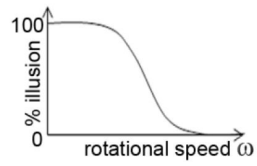


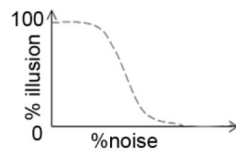
Fig. 5.
Intermediate frames showing the mask rotation with $\theta=20^\circ$



a



b



c

Fig. 6. The variation of illusion strength as a function of (a) rotational amplitude (b) rotational speed (c) amount of noise, See text for details

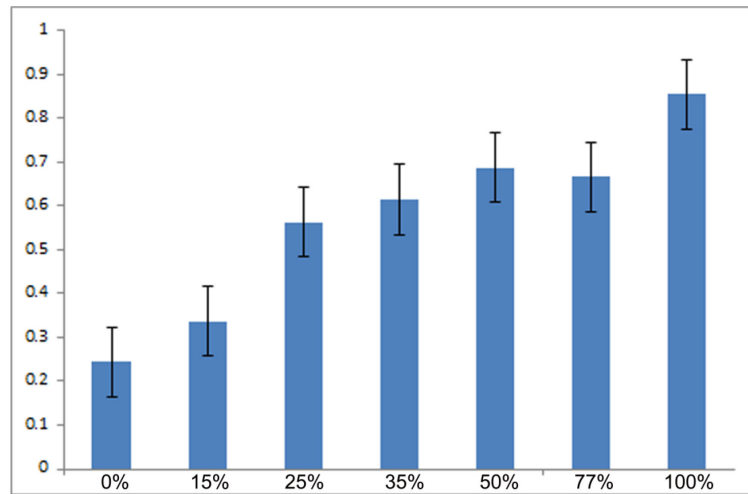


Fig. 7.

Each bar along the x axis indicates a stimulus with varying values of F (realistic texture) in percentages as 0%, 15%, 25%, 35%, 50%, 77%, and 100%. The height of each bar indicates the proportion of time that observers spent in the illusory percept during a 120-second trial.